Robust Pitch Control of a 1.5 MW Wind Turbine Using Integral Sliding Mode Control

Marcos de la Rosa
Computer Science Faculty
Complutense University of Madrid
Madrid, Spain
mdelar06@ucm.es

Matilde Santos
Institute of Knowledge Technology
Complutense University of Madrid
Madrid, Spain
msantos@ucm.es

Jesús Enrique Sierra-García
System Engineering and Automatic Control
University of Burgos
Burgos, Spain
jesierra@ubu.es

***Abstract*—This paper proposes a robust pitch control strategy for a 1.5 MW wind turbine operating in Region 3 using an Integral Sliding Mode Control (ISMC) approach. The control objective is to regulate the generated electrical power at its rated value under varying wind conditions. The controller is derived from a simplified rotor dynamic model and employs an integral sliding surface based on the power tracking error, eliminating the need for error differentiation while ensuring zero steady-state error. Unlike conventional sliding mode approaches, the proposed ISMC formulation combines the integral sliding surface with a local aerodynamic torque linearization, enabling the computation of practical pitch references through a first-order aerodynamic sensitivity approximation while employing a saturation-based switching law to reduce the discontinuity of the control action. The proposed strategy is evaluated under turbulent, sinusoidal, and sawtooth wind profiles and compared against a conventional PI pitch controller. Simulation results demonstrate significant improvements in power regulation performance and robustness, particularly under abrupt wind transients, achieving up to 95.03% RMSE reduction and 97.53% IAE reduction compared to the PI benchmark. Furthermore, the proposed approach effectively mitigates integral windup phenomena and maintains stable power tracking during sudden wind speed drops.**

***Index Terms*—Wind turbine control, sliding mode control, pitch control, renewable energy, nonlinear control**

I. Introduction

Wind energy is one of the most widely deployed renewable energy sources worldwide due to its low environmental impact and high scalability [1]. The continuous expansion of wind power installations has driven significant advances in turbine aerodynamics, power electronics, and control systems. Modern utility-scale wind turbines operate across different control regions depending on wind speed, enabling efficient energy capture while ensuring structural safety and grid compliance.

Wind turbine operation is typically divided into regions according to wind speed. In Region 2, the control objective is to maximize energy capture by maintaining the optimal tip-speed ratio. In contrast, in Region 3, where wind speed exceeds the rated value, the primary objective is to regulate the generated electrical power at its nominal level in order to prevent structural overloads and ensure safe operation of mechanical and electrical components [2]. Stable power regulation in this region is critical for both turbine reliability and grid stability.

Pitch control is the primary mechanism used to limit aerodynamic power in Region 3 [3]. Conventional pitch control strategies are commonly based on proportional–integral-derivative (PID) controllers due to their simplicity and industrial acceptance. However, wind turbine dynamics are highly nonlinear and strongly affected by turbulence and gusts. Under these conditions, linear controllers may exhibit degraded performance and integral windup phenomena, particularly during fast wind variations [4].

To overcome these limitations, nonlinear control techniques have been widely investigated. Among them, Sliding Mode Control (SMC) is well known for its robustness against parameter uncertainties and external disturbances [5] and has been successfully applied to wind energy systems for rotor speed and power regulation [6], [7].

Recent nonlinear control strategies beyond wind energy applications have also demonstrated strong robustness against uncertainties and disturbances [8]. In addition, fractional-order sliding mode control, experimental implementations on laboratory-scale wind systems, and robust nonlinear control of permanent magnet synchronous generator-based turbines have shown improved disturbance rejection capabilities [9]–[13].

Despite these advantages, classical sliding mode controllers suffer from chattering due to discontinuous control action and sensitivity to measurement noise when derivative terms are involved in the sliding surface. To address these issues, Integral Sliding Mode Control (ISMC) introduces an integral component in the sliding surface, eliminating steady-state error and avoiding numerical differentiation of measured signals, while preserving robustness to disturbances.

In this work, an ISMC strategy is proposed for pitch control of a 1.5 MW wind turbine operating in Region 3. The controller is derived from a simplified rotor dynamic model and employs a sliding surface based on the power tracking error and its integral. Furthermore, the required aerodynamic torque is mapped into a feasible pitch reference using a local aerodynamic linearization based on torque sensitivity with respect to blade pitch angle.

The main contributions of this paper are: (i) the development of an ISMC-based pitch control strategy for Region 3 operation, (ii) its analytical derivation from a simplified wind turbine model, (iii) the inclusion of a practical aerodynamic torque-to-pitch linearization for real-time implementation, and (iv) a comprehensive performance evaluation against a conventional PI controller under different wind scenarios.

The remainder of this paper is organized as follows. Section II describes the wind turbine model. Section III presents the proposed control design. Section IV reports simulation results and comparative analysis. Section V concludes the paper, and Section VI discusses future research directions.

II. Wind Turbine Model

The electrical power generated by the turbine can be written as

$$P_{out} = \eta_g N T_{hs} \omega_r \tag{1}$$

where η_g is the generator efficiency, N is the gearbox ratio, T_{hs} is the high-speed shaft torque and ω_r is the rotor angular velocity [12].

In Region 3 operation the generator operates under constant torque control, allowing these parameters to be considered constant. Differentiating the power expression yields

$$\dot{P}_{out} = (\eta_g N T_{hs})\dot{\omega}_r \tag{2}$$

The rotor dynamics can be described using a single-mass mechanical model [1]

$$J_r \dot{\omega}_r = T_a(\theta, v) - T_{ls} \tag{3}$$

where T_{ls} is the low-speed shaft torque, J_r is the equivalent rotor inertia, and T_a is the aerodynamic torque captured by the rotor as a function of the blade pitch angle θ and the wind speed v, given by:

$$T_a = \frac{1}{\omega_r}\left(\frac{1}{2}\rho\pi R^2 v^3 C_p(\lambda,\theta)\right) \tag{4}$$

where ρ is the air density, R is the rotor radius, v the wind speed and C_p the power coefficient.

Combining the mechanical and electrical dynamics leads to the overall plant model:

$$\dot{P}_{out} = \frac{\eta_g N T_{hs}}{J_r}(T_a - T_{ls}) \tag{5}$$

This expression represents the nonlinear plant dynamics that the proposed controller must regulate. The physical and operational parameters of the 1.5 MW wind turbine model used for the simulations are summarized in Table I.

TABLE I
Parameters of the 1.5 MW Wind Turbine Model

Parameter	Description	Value / Units
P_{rated}	Rated electrical power	1.5×10^6 W
R	Rotor radius	35 m
ρ	Air density	1.225 kg/m^3
N	Gearbox ratio	88
η_g	Generator efficiency	0.95
J_r	Equivalent rotor inertia	3.41×10^6 kg·m^2
T_{hs}	Rated high-speed shaft torque	8376.58 N·m
K_θ	Pitch actuator gain	1.43
τ_θ	Pitch actuator time constant	0.36 s

III. ISMC Control Architecture

The primary objective of the proposed control scheme is to maintain the generated output power, P_{out}, at its rated value, P_{rated}, by manipulating the blade pitch angle, θ_{ref}, under stochastic wind speed disturbances, v. The overall architecture is illustrated in Fig. 1.

As shown in the diagram, the control system is composed of two main stages: the ISMC Core Law and the Torque-to-Pitch Aerodynamic Linearization.

To facilitate the control design, the constant parameter K_p is defined as:

$$K_p = \frac{\eta_g N T_{hs}}{J_r} \tag{6}$$

The power tracking error is defined as:

$$e(t) = P_{rated} - P_{out}(t) \tag{7}$$

Taking the derivative of the error and substituting the plant dynamics yields the error dynamics:

$$\dot{e} = -K_p(T_a - T_{ls}) \tag{8}$$

This expression relates the evolution of the power error directly to the aerodynamic torque.

To process this error and compute the final pitch command, the control architecture is organized into two main stages, which are developed in the following subsections. The first stage, referred to as the ISMC Core, includes the formulation of the integral sliding surface and the derivation of the control law. The second stage addresses the torque-to-pitch aerodynamic conversion required to obtain the pitch reference.

A. Integral Sliding Surface

To avoid amplifying measurement noise when differentiating the error, an integral sliding surface is proposed, which guarantees zero steady-state error:

$$s(t) = e(t) + k_i \int_0^t e(\tau)\, d\tau \tag{9}$$

Differentiating the sliding surface yields

$$\dot{s}(t) = \dot{e}(t) + k_i e(t) \tag{10}$$

Substituting the error dynamics gives

$$\dot{s}(t) = -K_p(T_a - T_{ls}) + k_i e(t) \tag{11}$$

If the controller forces the trajectories to remain on the sliding surface ($s(t) = 0$), then $\dot{s}(t) = 0$, which leads to the reduced-order error dynamics

$$\dot{e}(t) = -k_i e(t) \tag{12}$$

This corresponds to a stable first-order system, ensuring exponential convergence of the power tracking error to zero.

B. Control Law

The control objective is to design a control law that forces the system trajectories to reach and remain on the sliding surface despite disturbances and modeling uncertainties.

The control action is decomposed into two components:

$$u = u_{eq} + u_{sw} \tag{13}$$

where u_{eq} represents the equivalent control that compensates the nominal plant dynamics, and u_{sw} is the switching control responsible for enforcing the sliding condition.

A Lyapunov-based reaching law with boundary layer is defined as:

$$\dot{s} = -K_{sw}\,\text{sat}\left(\frac{s}{\Phi}\right) \tag{14}$$

where K_{sw} is a strictly positive switching gain and Φ defines the boundary layer thickness. The use of the saturation function replaces the discontinuous sign function, resulting in a smoother control action in the torque domain.

Considering the Lyapunov candidate $V(s) = \frac{1}{2}s^2$, its time derivative becomes:

$$\dot{V} = -K_{sw}s \cdot \text{sat}\left(\frac{s}{\Phi}\right) \tag{15}$$

Since $K_{sw} > 0$ and $s \cdot \text{sat}(s/\Phi) \geq 0$ for all s, it follows that $\dot{V} \leq 0$, guaranteeing stability of the reaching condition and convergence to the sliding manifold.

Equating the previous expression with the sliding surface dynamics leads to

$$-K_p(T_a - T_{ls}) + k_i e = -K_{sw}\,\text{sat}\left(\frac{s}{\Phi}\right) \tag{16}$$

Solving for the required aerodynamic torque, the total control law is defined by:

$$T_{a,req} = \underbrace{T_{ls} + \frac{k_i e}{K_p}}_{u_{eq}} + \underbrace{\frac{K_{sw}}{K_p}\text{sat}\left(\frac{s}{\Phi}\right)}_{u_{sw}} \tag{17}$$

The equivalent term compensates nominal dynamics, while the switching term enhances robustness against wind disturbances and model uncertainties.

The saturation function in u_{sw} reduces high-frequency switching effects in the control torque, avoiding discontinuous control actions at the control law level.

C. Torque-to-Pitch Aerodynamic Linearization

Since the actuator can only manipulate the blade pitch angle, the required aerodynamic torque $T_{a,req}$ is mapped into a pitch reference θ_{ref} using a local aerodynamic linearization [4].

The mapping is based on a first-order approximation around the current operating point:

$$\Delta\theta = \frac{T_{a,req} - T_a}{\partial T_a / \partial\theta} \tag{18}$$

The sensitivity of the aerodynamic torque with respect to pitch is computed as:

$$\frac{\partial T_a}{\partial\theta} = \left(\frac{1}{2}\rho\pi R^2 \frac{v^3}{\omega_r}\right)\frac{\partial C_p}{\partial\theta} \tag{19}$$

The derivative of C_p is obtained numerically from aerodynamic lookup tables of the turbine.

The final pitch reference is given by:

$$\theta_{ref} = \theta + \Delta\theta \tag{20}$$

The aerodynamic linearization is updated at each sampling interval using a discrete lookup-table-based scheme, allowing adaptation to varying operating conditions in Region 3.

This linearization provides a practical torque-to-pitch mapping suitable for real-time implementation in wind turbine systems.

The resulting pitch reference θ_{ref} remains sufficiently smooth for actuator implementation. However, under highly turbulent wind conditions, small high-frequency variations may still appear due to rapid changes in aerodynamic operating points.

IV. Results

The proposed controller was evaluated using a simulation model of a 1.5 MW wind turbine. To thoroughly assess the dynamic response and robustness of the ISMC against an industrial PI controller, three distinct wind scenarios were considered: a realistic turbulent wind profile, a continuous sinusoidal wave, and a sawtooth profile.

Additional tuning experiments using optimization-based PI adjustment showed that the PI performance can be improved for specific wind profiles, particularly under turbulent conditions. However, these gains resulted in degraded performance under other wind scenarios, whereas the proposed ISMC maintained more consistent behavior across all evaluated operating conditions.

For benchmarking purposes, a conventional fixed-gain PI pitch controller is selected as the baseline, since PI-based pitch regulation remains one of the most widely used industrial strategies for Region 3 wind turbine operation due to its simplicity, reliability, and low computational cost. The objective of this comparison is not to evaluate different sliding mode variants, but to assess the robustness and transient performance of the proposed ISMC against a representative industrial controller under identical operating conditions. The PI controller is implemented with empirically tuned gains $K_p = -2 \times 10^{-5}$ and $K_i = -5 \times 10^{-6}$, ensuring stable Region 3 operation, acceptable power tracking, and limited steady-state error.

A. Turbulent Wind Profile

Under random and turbulent wind conditions, the controller must reject continuous stochastic disturbances. As shown in Fig. 2, the ISMC efficiently suppresses power overshoots and demonstrates near-perfect tracking capabilities compared to the PI controller, which exhibits significant power fluctuations.

The tracking superiority is further evidenced in Fig. 3. Measuring the Integral of Absolute Error (IAE), the PI controller accumulates a significantly larger error, whereas the ISMC drastically reduces this metric, confirming the effectiveness of the integral sliding surface coupled with the Lyapunov switching logic.

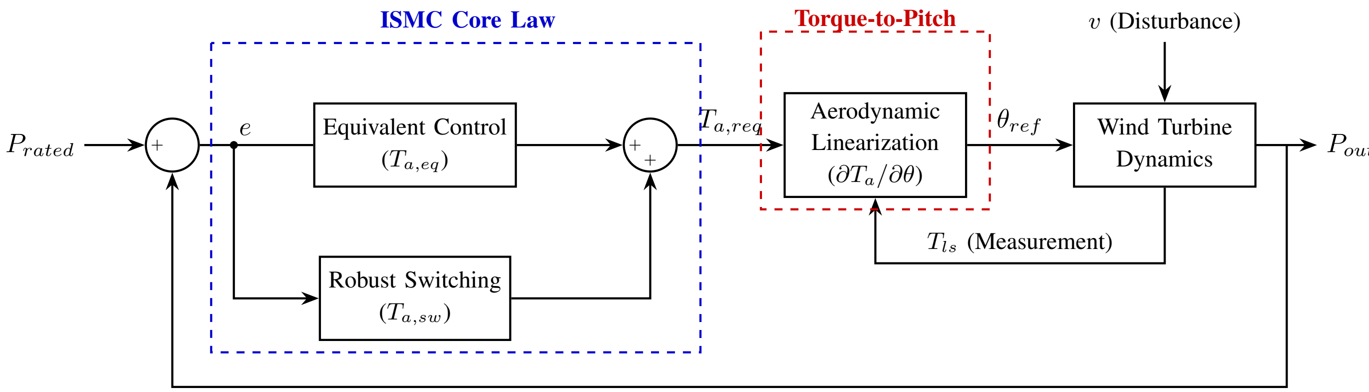

Fig. 1. Detailed architecture of the proposed Integral Sliding Mode Control scheme. The ISMC Core Law processes the error e to generate $T_{a,req}$, which is then translated via aerodynamic linearization into the pitch reference θ_{ref}.

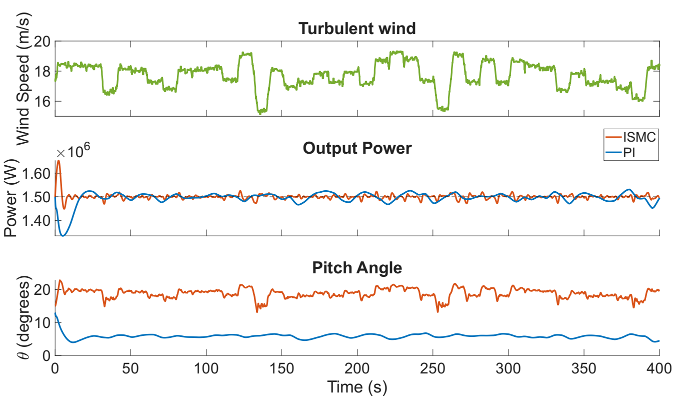

Fig. 2. Dynamic performance of the proposed ISMC and the baseline PI controller under a turbulent wind profile, illustrating the wind speed variations, output power regulation, and pitch angle actuation.

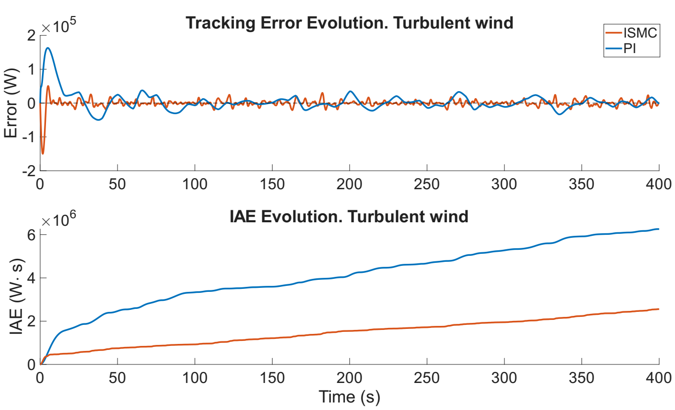

Fig. 3. Instantaneous power tracking error and Integral of Absolute Error (IAE) evolution for the ISMC and PI controllers under turbulent wind conditions.

B. Sinusoidal Wind Profile

To evaluate the tracking phase lag, a sinusoidal wind profile was applied. Fig. 4 details the generated power response, where the ISMC seamlessly tracks the reference without the temporal lag characteristic of the PI controller. Fig. 5 demonstrates the minimal error accumulation of the proposed strategy under continuous smooth variations.

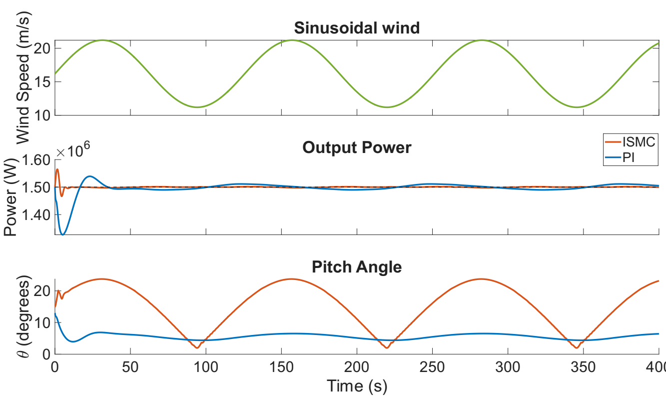

Fig. 4. Continuous tracking performance of the evaluated controllers under a sinusoidal wind speed profile, detailing the wind wave, generated power response, and pitch angle adjustments.

C. Sawtooth Wind Profile

The sawtooth profile tests the controllers against a critical aerodynamic phenomenon: constant acceleration followed by a sudden wind drop. As illustrated in Fig. 6, the sudden drop completely saturates the PI controller (integral windup), causing a severe loss of power tracking. In contrast, the ISMC rapidly recovers. The error evolution in Fig. 7 highlights the robustness of the nonlinear switching term, preventing windup and maintaining stability.

D. Quantitative Analysis

Table II summarizes the quantitative metrics (RMSE and IAE) for all evaluated profiles. The ISMC achieves an overwhelming improvement across all scenarios. Notably, under the sawtooth profile, the ISMC reduces the RMSE by 95.03% and the IAE by 97.53%, proving its superiority in handling severe aerodynamic transients.

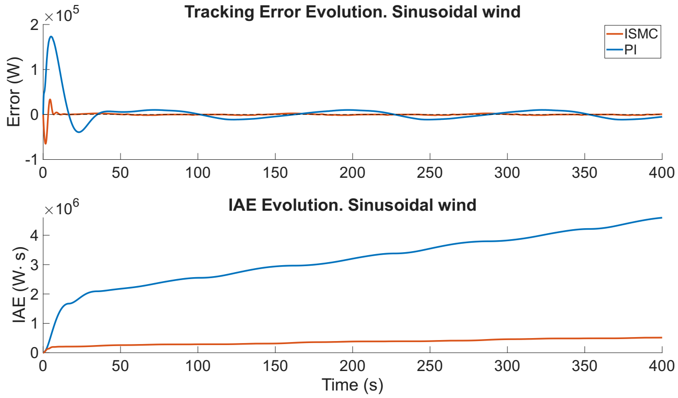

Fig. 5. Evolution of the tracking error and cumulative IAE during the sinusoidal wind profile, demonstrating the superior tracking capability and reduced lag of the proposed ISMC.

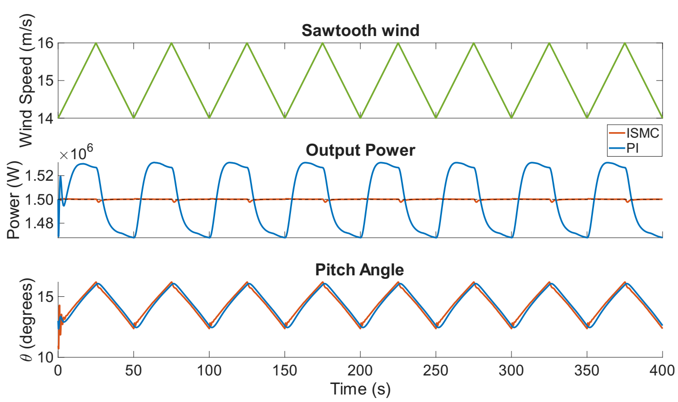

Fig. 6. Dynamic performance of the ISMC and PI controllers under a sawtooth wind speed profile, illustrating the system's response to constant wind acceleration followed by sudden drops.

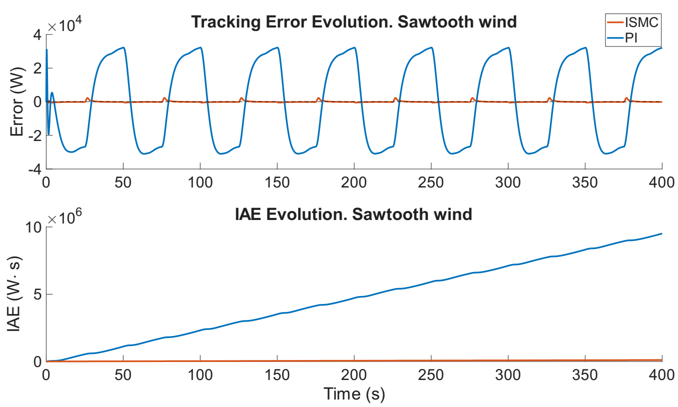

Fig. 7. Tracking error evolution and cumulative IAE under the sawtooth wind profile, demonstrating the ISMC's robustness and rapid recovery against sudden wind speed drops compared to the PI controller.

TABLE II
QUANTITATIVE PERFORMANCE COMPARISON BETWEEN ISMC AND PI CONTROLLERS

Wind Profile	Metric	PI	Proposed ISMC	Improvement
Sinusoidal	RMSE (W)	22434.45	4131.89	81.58%
	IAE (Ws)	5.59×10^6	5.21×10^5	90.67%
Sawtooth	RMSE (W)	20208.07	1005.04	95.03%
	IAE (Ws)	5.85×10^6	1.44×10^5	97.53%
Turbulent	RMSE (W)	18566.40	7641.93	58.84%
	IAE (Ws)	4.17×10^6	2.03×10^6	51.35%

These results confirm the robustness of the proposed ISMC strategy under different wind disturbances and highlight its effectiveness in preventing integral windup phenomena compared to classical PI control.

The lower relative improvement observed under turbulent wind conditions is mainly associated with the high-frequency stochastic components present in the wind profile. Since the aerodynamic torque-to-pitch linearization is updated at every sampling interval using lookup-table-based sensitivity calculations, rapid variations in the operating point may produce more active pitch references under turbulent conditions.

This behavior is reflected in the control effort analysis based on a normalized root mean square (RMS) index of the pitch rate, computed with respect to a reference pitch-rate value used for normalization. Under severe transient conditions such as the sawtooth wind profile, the ISMC reduces the normalized pitch effort index compared to the PI baseline (0.3097 vs. 0.3553), indicating smoother control action during abrupt wind variations. Under turbulent wind conditions, however, the ISMC exhibits a higher activity index (0.1000 vs. 0.0404), which is consistent with its active rejection of high-frequency stochastic disturbances and the faster updates of the aerodynamic linearization.

This increased actuator activity should not be interpreted as classical sliding-mode chattering. The saturation function smooths the switching action at the torque-control level and avoids discontinuous control signals. Nevertheless, residual high-frequency components may still appear in the pitch reference due to rapid aerodynamic operating point variations under turbulent wind conditions.

Overall, the proposed ISMC still achieves significant improvements over the PI baseline, confirming its robustness under stochastic wind disturbances while maintaining bounded pitch actuation.

V. CONCLUSIONS

This paper has presented an Integral Sliding Mode Control (ISMC) strategy for pitch regulation of a 1.5 MW wind turbine operating in Region 3. By formulating an integral sliding surface based on the power tracking error, the proposed controller avoids the numerical differentiation of measured signals while ensuring zero steady-state error [14]. This feature improves robustness against disturbances commonly present in wind energy systems.

The required aerodynamic torque was converted into a feasible pitch command through a local aerodynamic linearization, enabling practical implementation of the proposed control strategy within a standard pitch-actuated wind turbine architecture.

The controller was evaluated under turbulent, sinusoidal, and sawtooth wind profiles and compared with a conventional fixed-gain PI controller. The results showed consistent improvements in power regulation performance across all scenarios. In particular, under severe transient conditions such as sudden wind speed drops, the ISMC prevented integral windup and preserved stable power tracking. Quantitatively, the proposed method achieved reductions above 95% in both RMSE and IAE under the most demanding scenario, highlighting its effectiveness for robust power regulation in Region 3.

The comparison was conducted against a representative industrial fixed-gain PI baseline under identical operating conditions. Therefore, the objective was not to evaluate different sliding mode variants, but to assess the improvement provided by the proposed ISMC structure over a conventional pitch control strategy.

The present study is based on a simplified single-mass drivetrain model and does not include drivetrain torsional flexibility, aeroelastic effects, grid-side converter dynamics, or explicit sensor noise modeling. In addition, the controller was validated exclusively in Region 3 operation, while the transition between Regions 2 and 3 was not addressed. Therefore, the obtained results should be interpreted within the limitations of the adopted reduced-order framework.

VI. Future Work

Future research will extend the proposed ISMC framework toward more realistic and demanding operating conditions. First, higher-fidelity wind turbine models will be considered, including drivetrain torsional flexibility, aeroelastic blade dynamics, converter-side interactions, and multi-megawatt offshore reference turbines such as 15 MW systems. This will allow the assessment of the controller under increased inertia, structural flexibility, and environmental complexity.

Second, the aerodynamic linearization strategy will be improved through adaptive and multi-rate update schemes to increase accuracy under fast turbulent wind variations and large operating point deviations. Since the current approach relies on lookup tables under ideal blade conditions, future work will also assess robustness against aerodynamic uncertainties caused by blade erosion or icing.

Third, the proposed controller will be benchmarked against advanced nonlinear strategies, including higher-order and hybrid sliding mode controllers, as well as industry-standard gain-scheduled PI controllers and the NREL reference wind turbine controller. Finally, integration with data-driven techniques such as Reinforcement Learning [15], [16] will be explored to enable adaptive tuning of sliding surface parameters and switching gains, while also considering secondary objectives such as structural load mitigation.

Acknowledgment

This work has been partially supported by the Spanish Ministry of Science and Innovation under the projects MCI/AEI/FEDER number PID2021-123543OB-C21 and PID2024-155653OB-C21.

References

[1] F. D. Bianchi, H. De Battista, and R. J. Mantz, *Wind Turbine Control Systems: Principles, Modelling and Gain Scheduling Design*. Berlin, Germany: Springer, 2006.

[2] E. Muljadi and C. P. Butterfield, "Pitch-controlled variable-speed wind turbine generation," *IEEE Transactions on Industry Applications*, vol. 37, no. 1, pp. 240–246, 2001.

[3] A. M. S. Hwas and R. Katebi, "Wind turbine control using PI pitch angle controller," *IFAC Proceedings Volumes*, vol. 45, pp. 241–246, 2012.

[4] E. Ren, L. Li, J. Brindley, and L. Jiang, "Nonlinear PI control for variable pitch wind turbine," *Control Engineering Practice*, vol. 50, pp. 84–94, 2016.

[5] S. M. Mozayan, M. Saad, H. Vahedi, H. Fortin-Blanchette, and M. Soltani, "Sliding mode control of PMSG wind turbine based on enhanced exponential reaching law," *IEEE Transactions on Industrial Electronics*, vol. 63, no. 10, pp. 6148–6159, 2016.

[6] L. Colombo, M. L. Corradini, G. Ippoliti, and G. Orlando, "Pitch angle control of a wind turbine operating above the rated wind speed: A sliding mode control approach," *ISA Transactions*, vol. 96, pp. 95–102, 2020.

[7] S.-H. Lee, Y. Joo, J. Back, J.-H. Seo, and I. Choy, "Sliding mode controller for torque and pitch control of PMSG wind power systems," *Journal of Power Electronics*, vol. 11, no. 3, pp. 342–349, 2011.

[8] G. E. M. Abro, S. A. Memon, A. A. Hoshu, and N. Saeed, "Latency-aware attitude control of underactuated quadrotor UAVs using barrier Lyapunov and fuzzy Padé approximation," *Scientific Reports*, 2026.

[9] N. B. Son, T. U. Le Anh, M. T. Hai, and N. T.-T. Vu, "Pitch angle control for variable speed wind turbine using fractional-order sliding mode control," *Journal of Engineering Science and Technology*, vol. 21, no. 1, pp. 66–83, 2026.

[10] A. Kumar, P. Surana, and A. Dey, "Performance evaluation of a lab-scale Type-IV WECS with sliding mode controller by emulating wind turbine," *IEEE Journal of Emerging and Selected Topics in Industrial Electronics*, 2026.

[11] C. Acosta Lúa, D. Bianchi, S. Martín Baragaño, M. Di Ferdinando, and S. Di Gennaro, "Robust nonlinear control of a wind turbine with a permanent magnet synchronous generator," *Energies*, vol. 16, no. 18, p. 6649, 2023.

[12] M. Arabi, Y. Zennir, H. Bounezour, M. de la Rosa, J. E. Sierra-García, and M. Santos, "Optimized sliding mode control of a PMSG-based wind turbine using the Grey Wolf Optimizer," 2025, under review.

[13] B. Yang, T. Yu, H. Shu, Y. Zhang, J. Chen, Y. Sang, and L. Jiang, "Passivity-based sliding-mode control design for optimal power extraction of a PMSG based variable speed wind turbine," *Renewable Energy*, vol. 119, pp. 577–589, 2018.

[14] M. J. Morshed and A. Fekih, "Design of a chattering-free integral terminal sliding mode approach for DFIG-based wind energy systems," *Optimal Control Applications and Methods*, vol. 41, pp. 1718–1734, 2020.

[15] J. E. Sierra-García and M. Santos, "Performance analysis of a wind turbine pitch neurocontroller with unsupervised learning," *Complexity*, 2020.

[16] E. Muñoz-Palomeque, J. E. Sierra-García, and M. Santos, "Intelligent control techniques for maximum power point tracking in wind turbines," *Revista Iberoamericana de Automática e Informática Industrial*, vol. 21, pp. 193–204, 2024.